Clay minerals in the Pliocene−Quaternary sediments of the southern Yangtze coast, China: Sediment sources and palaeoclimate implications

Jing Chen[1], Zhang-Hua Wang[1, *], Tao-Yuan Wei[1], Bao-Cheng Zhao[2], Zhong-Yuan Chen[1]

1. State Key Laboratory of Coastal and Estuarine Research, East China Normal University, Shanghai 200062, China
2. Shanghai Geological Survey, Shanghai 200072, China

Abstract Clay mineralogy was used as an indicator of the sediment source and prevailing climate and five suites (I−V) were identified throughout the borehole. Smectite was dominant in the bottom suite of the borehole, indicating the sediment was mainly derived from the local basalt when the study area stood as uplands during the Pliocene. The sharp reduction of smectite in suites II and III (Early Pleistocene) reflects a broader sediment provenance due to neo-tectonic subsidence of the study area. Significant climate fluctuations are indicated by distinct variations in the ratios of illite versus smectite and kaolinite, and by the illite crystallinity in suites II and IV. Especially the suite IV, which forms mottled muddy sediments that underwent pedogenesis, possibly represents glacial/interglacial cycles during the Mid-Pleistocene climate transition (MPT). The rare presence of smectite in suite V which formed during the Late Quaternary suggests a significant contribution of fine-grained sediment derived from the upstream of the Yangtze catchment. Such changes in sediment sources are consistent with the evolution of regional sedimentary environments, which evolved towards an open coast/deltaic setting and imply that the study area became the depositional basin of the Yangtze fine-grained sediment due to the final submergence of the Wu-Nan-Sha and Fukien-Reinan Massifs since the Late Quaternary.

Key words smectite, neo-tectonic subsidence, Mid-Pleistocene climate transition, Yangtze depocenter, Pliocene−Quaternary, southern Yangtze coast

1 Introduction

The Late Cenozoic sediment sources and associated environmental evolution in the southern Yangtze coastal area of eastern China have been debated because of its close relationship with the uplift of the eastern Qinghai-Tibetan Plateau and the development of the east China marginal sea (Clark *et al.*, 2004; Wang, 2004; Yang *et al.*, 2006a; 2006b; Chen *et al.*, 2009). In the past decades, many studies have been carried out in this area regarding the neo-tectonic subsidence, sedimentary environment and stratigraphy, sediment provenance, palaeoclimatic change, marine transgression and regression (Lin *et al.*, 1989; Chen and Stanley, 1995; Chen *et al.*, 1997; Wang *et al.*, 2005, 2014; Yang *et al.*, 2006a; 2006b; Chen *et al.*, 2009). Recently, analyses focused on tracing the sediment sources by diagnostic indices including geochemical elements and heavy minerals from the upstream of the Yangtze catchment. For example, Yang *et al.* (2006b) used geochemical elements

and monazite age patterns to identify the variation of sediment sources since the Late Cenozoic. Their results suggested that the palaeo-Yangtze River changed its drainage basin from a local small one to a large river originating on the eastern Qinghai-Tibetan Plateau during the Early Pleistocene. Meanwhile, Chen *et al.* (2009) linked suites of heavy minerals in the Late Cenozoic sediments of the southern Yangtze coast to different source rocks in the catchment and argued that the heavy minerals from the upper catchment did not appear until the Late Pleistocene. To examine these different opinions, more studies are needed considering the nature of the coastal sediments which reflect both the evolution of the sedimentary basin and changes in sediment sources.

Clay minerals and their distributions have been widely used for the reconstruction of palaeoenvironments and palaeoclimates (Vanderaveroet *et al.*, 1999; Pehlivanoglou *et al.*, 2000; Perederij, 2001; Madhavaraju *et al.*, 2002; Liu *et al.*, 2003, 2004). Kaolinite, smectite, chlorite and illite are the major four proxies of clay minerals to test palaeoenvironmental hypotheses. Kaolinite is a product of strong chemical weathering in a high-temperature and high-moisture climate setting (Chamley, 1989; Velde, 1992). Smectite indicates either an alkaline weathering environment, regardless of what the parent rock is, or basalt bedrock as the sediment provenance (Chamley, 1989; Aoki and Kohyama, 1991; Velde, 1992; Naidu *et al.*, 1995; Wahsner *et al.*, 1999; Viscosi-Shirley *et al.*, 2003). Chlorite and illite tend to be linked to a cold and/or temperate climate regime, where physical weathering predominates (Velde, 1992).

Previous study revealed that clay mineral assemblages differ clearly in the suspended sediments from different rivers of eastern China. Smectite decreases from the Yellow River of northern China to the Pearl River of southern China, in combination with an increase of kaolinite. The diagnostic clay mineral in the Yellow River is smectite; in the Yangtze River it is illite, and in the Min and Pearl River it is kaolinite (Yang, 1988; He and Liu, 1997; Ma *et al.*, 2010). Besides, the ratio of illite to smectite has been proposed as a provenance proxy for the Yellow and Yangtze Rivers (Fan *et al.*, 2001).

Therefore, the present study aims to examine the temporal distribution of four clay minerals in a Late Cenozoic borehole, coded PD from the coast of the southern Yangtze delta (Figure1), so that to discuss the changes of sediment sources through time and also to reveal possible relationship with climate change. This will help to better understand the evolution of the southern Yangtze coast and associated eastern China marginal sea.

2 Geological setting

The southern Yangtze delta plain is located on the Wu-Nan-Sha Massif that collided with the Fukien-Reinan Massif during the Late Mesozoic (Wageman *et al.*, 1970; Guo *et al.*, 1997; Figure 2A). The East China Sea (ECS) Shelf Depression initiated coincidently with the collision (Figure 2A). Several separate terrestrial basins were also formed in eastern China, including the Subei-Southern Yellow Sea (YS), Qingdong, Northern YS, and the Bohai Sea. The outer ECS was formed during the Himalayan movement of the Neogene, as the result of tensional spreading of the back-arc basin. The inner ECS shelf, however, was still dominated by the Fukien-Reinan Massif. The Cenozoic sediment is generally over 1500 m thick in these basins (Wageman *et al.*, 1970; Jin, 1992). In contrast, the total sediment thickness is generally less than 1000 m where it overlies the basement of the Wu-Nan-Sha and Fukien-Reinan Massifs. For the present southern Yangtze coast, the sediment thickness over the bedrock is mostly <200 m in the western and southern areas and 300−500 m in the east and north, with several deep and narrow valleys to the northeast (Zhang *et al.*, 2008; Figure 2B). Previous studies also show that most (200−450 m) unconsolidated sediments date from the Quaternary, with thinner (<50 m thick) Pliocene deposits underneath in local basins (Chen and Stanley, 1995; Chen *et al.*, 1997). The Wu-Nan-Sha and Fukien-Reinan Massifs started to subside in response to the strong uplift of the Qinghai-Tibetan Plateau, and as a result led to the coalescence of the ECS and the southern YS during the Quaternary (Guo *et al.*, 1997).

3 Materials and methods

Sediment borehole PD, 365 m long, was recovered from the southern Yangtze delta coast, ~5 km inland from the shoreline in 2001 (Figure 1). The borehole was obtained using a rotary rig and the bedrock (basalt) of Miocene age (Shanghai Geological Survey, 2001) was reached. On-site sediment description was made during the coring. Detailed sediment logging was carried out in the laboratory when splitting the core samples, including sediment lithology, bedding, fauna fossils, plant fragments/root traces, and nodule distribution.

The sediments of borehole PD were dated palaeomagnetically (Chen *et al.*, 2009). In the present study, we incorporate four quartz-rich samples for electron spin resonance (ESR) dating by using an ECS−106 ESR spec-
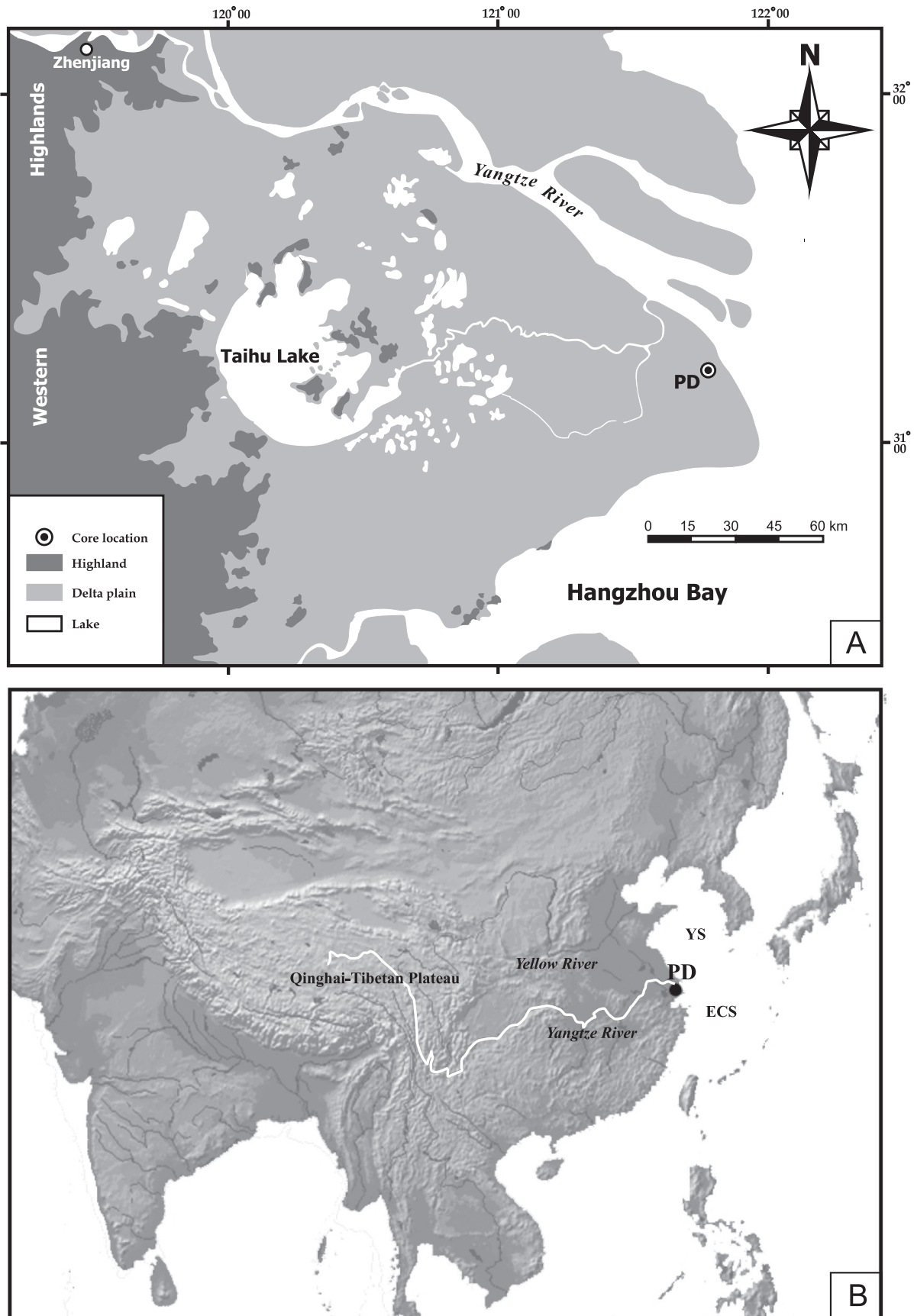
Jing Chen *et al.*: Clay minerals in the Pliocene−Quaternary sediments of
the southern Yangtze coast, China: Sediment sources and
palaeoclimate implications   299

Figure 1   Location of borehole PD on the southern Yangtze coast. A−The Yangtze delta; B−East Asia and marginal seas; YS−Yellow Sea, ECS−East China Sea.

trometer (Bruker), and two organic-rich samples for conventional radiocarbon dating in the Qingdao Institute of Marine Geology, China Geological Survey (Table 1). Besides, one sample was taken for OSL dating, which was conducted using Littlemore OSL/TL reader type 733 with a $^{90}Sr/^{90}Y$ beta source in the Institute of Hydrogeology and Environmental Geology, Chinese Academy of Geological Science (Table 1).

Grain size analysis, microfossil (Foraminifera and Ostracoda) identification and interpretation of the sedimentary environment have been reported for this borehole PD previously (Wang *et al.*, 2005; Chen *et al.*, 2009; Figure 3). Here we summarize the stratigraphy in Table 2.

Clay mineral analysis was conducted for 63 samples, selected on the basis of lithologic changes in the section. Deflocculation of clays was carried out by succes-
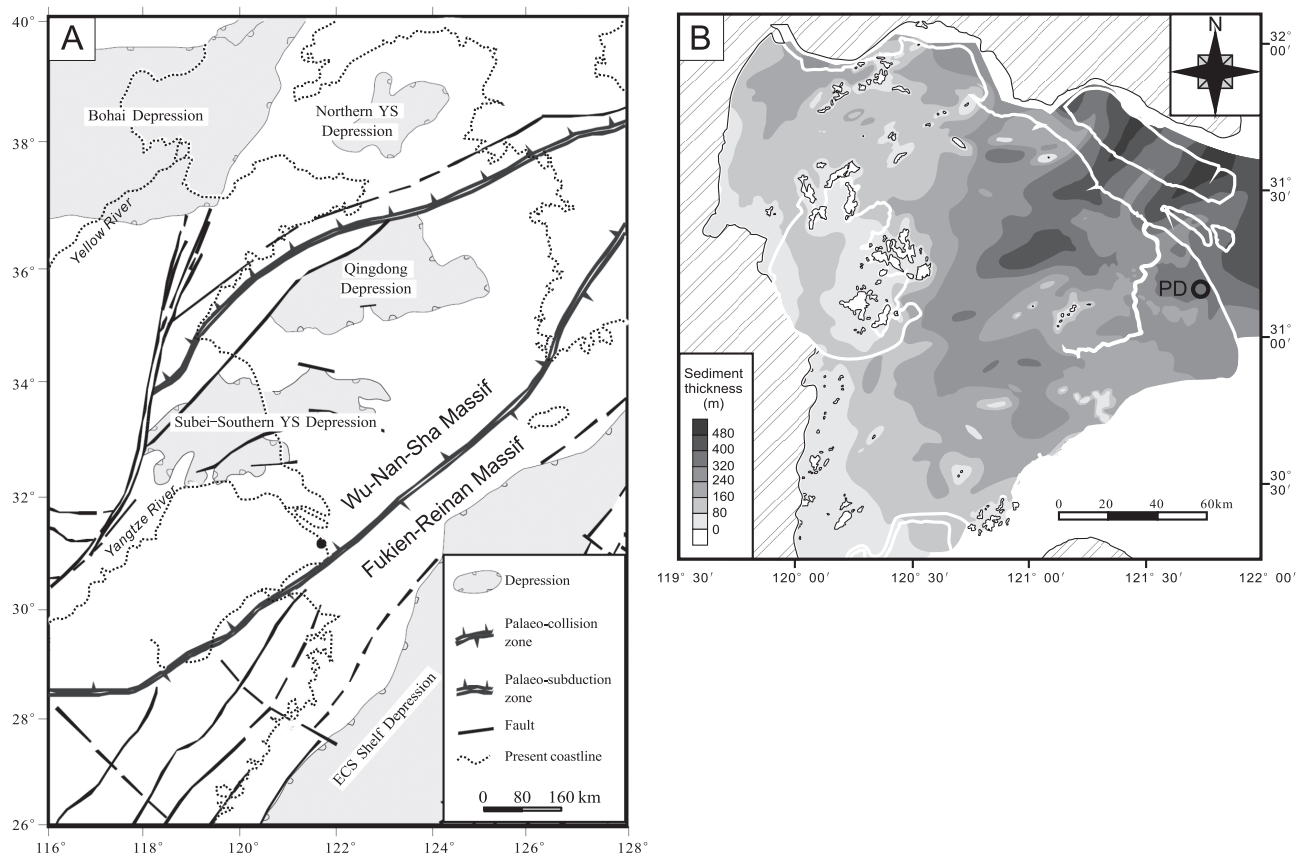

Figure 2 A−Tectonic framework of the eastern China and marginal seas, showing major depressions and the Wu-Nan-Sha and Fukien-Reinan Massifs (after Guo *et al.*, 1997); B−Isopach map of the Late Cenozoic sediments in the southern Yangtze coastal area, showing the relief of the bedrock surface (after Zhang *et al.*, 2008).

Table 1   Radiocarbon, OSL and ESR dating results.

Borehole depth (m)	Lithology	Dating method	Age (ka)
18.5−18.7	Dark grey mud	^{14}C	8.78±0.55
23.4−23.5	Dark grey mud	^{14}C	9.15±0.25
112.3−112.4	Bluish grey silty clay	OSL	116.4±11.25
193	Grey gravelly sand	ESR	984.0
222.5	Grey gravelly sand	ESR	1040.1
247.5	Light grey fine sand	ESR	1266.0
264.6	Light greyey yellow silty sand	ESR	1418.0

Vol. 3 No. 3

Jing Chen *et al*.: Clay minerals in the Pliocene−Quaternary sediments of
the southern Yangtze coast, China: Sediment sources and
palaeoclimate implications

301

Table 2   Stratigraphy of borehole PD, including lithology, grain size, microfossils, and interpretation of sedimentary environment.

Core depth (m)	Description of lithology	Mean grain size (φ)	Occurrence of foraminifers and ostracods	Interpretation of sedimentary environment
0−29.4	Clayey silt and silty clay.	4.30−7.30	Marine fossils abundant	Estuary to delta
29.4−95	Silt dominates, two thin layers of muddy sand with a few gravels in the lower section.	2.01−7.55	Marine fossils abundant in the upper section and rare in the lower section	Open coast
95−152	Mottled muddy sediment in the lower section, fining-upward gravelly coarse to medium sand in the upper section, capped by fine sand and silt.	0.15−7.66	Freshwater, ostracod fossils present	River channel and flood plain
152−289	Five thick fining-upward cycles; each cycle constitutes gravelly coarse to medium sand at the bottom, fine-grained muddy on the top. Pebbles (5−8 cm in diameter) above 248 m.	−0.50−4.71	A few freshwater ostracod fossils appear in the top mud	River channel
289−354.3	Several fining-upward cycles, in each cycle, thick or thin layers of coarse to medium sand with clay and gravel at the bottom, thin silty clay on the top. Gravels are angular to subangular, with weathered basalt fragment at the bottom.	−0.22−8.26	None	Alluvial fan

sive washing with distilled water after adding H_2O_2 and 10% HCl. Particles less than 0.002 mm were separated by precipitation according to Stokes′ Law and centrifugation. X-Ray diffraction (XRD) measurements were performed under 3 conditions separately, air-dried, ethylene glycolated for 12 h, and heating at 550 ºC for 2 h on the Philips X′pert MPD device, using a CuKα radiation and Ni filter, under a voltage of 35 kV and an intensity of 25 mA. Goniometer scans were run from 3º to 32º at 2θ with a step size of 0.02º.

For the semi-quantitative estimation of the clay minerals, the peak area was not used because of the possible overlapping of individual clay reflections (Thorez, 1985). Instead, we measured the peak intensity of the basal reflections of smectite (17 Å), illite (10 Å), and kaolinite/chlorite (7 Å) on the glycolated curve. The kaolinite/chlorite ratio was further calculated based on the peak intensities at 3.57 Å versus 3.54 Å and was then used to determine the proportions of the 7 Å peak intensity for both minerals. Percentages were finally obtained for the above 4 clay minerals using the weight factor of Biscaye (1965). Considering the relatively stable occurrence of illite throughout the borehole sediments, illite crystallinity, indicated here as H_W (half-peak-width of the 10Å peak) was calculated for each sample. The higher Hw is, the sharper the peak of illite, indicating better crystallinity.

4   Chronology

It is somewhat difficult to apply the chronology of pal-
aeomagnetism to borehole PD, because of frequent occurrences of thick layers of coarse sediment, especially in the lower section of the core (Figure 3). Borehole PD was hence compared with adjacent borehole PD99 (Yang *et al.*, 2006a, 2006b), in terms of both sediment cyclicity and palaeomagnetism. As a result, the Brunhes/Matayama (B/M) and Matayama/Gauss (M/G) boundaries of PD were revised at a core depth of ~152 m and ~289 m, respectively (Figure 4). The ESR age of 984.0 ka BP at a core depth of 193 m is consistent with the palaeomagnetic results, but the ESR ages at larger depth are much younger than the palaeomagnetic ages (Table 1). Considering the OSL, ^{14}C, and palaeomagnetic ages, the base of the Holocene is suggested to be at a core depth of 29.4 m, the Late Pleistocene is identified as being between 29.4 and 103 m, and the Mid-Pleistocene between 103 and 152 m (Table 1, Figure 4). The M/G boundary is used as the base of the Early Pleistocene, so as to be consistent with previous cores (Lin *et al.*, 1989; Chen *et al.*, 1997; Yang *et al.*, 2006a, 2006b).

5   Clay mineral distribution

Five clay mineral suites are distinguished in borehole PD (I−V, from bottom to top; Figure 5), each being characterized as follows.

Suite I (358−287 m)

Smectite dominates in the Pliocene sediment, ranging from 51% to 100% (74% on average) with an upward-increasing trend (Figure 5). Illite is secondary, decreasing upward from 45% to 0%, with an average of 21%. Kao-
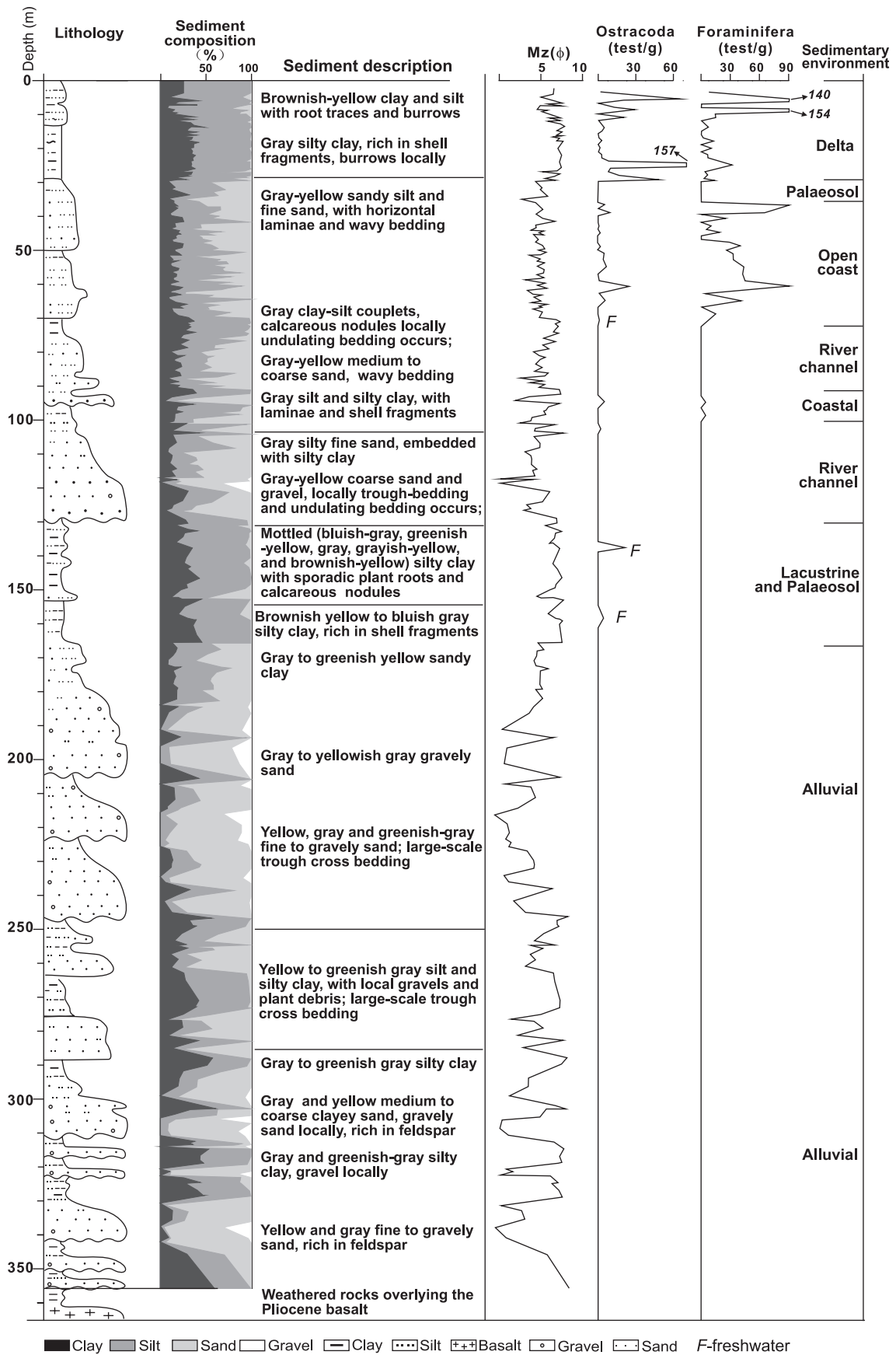
Figure 3 Comprehensive sediment profile of borehole PD, including lithology, grain size, microfossils and interpretation of the sedimentary environment. *F* beside the ostracod curve represents freshwater species.
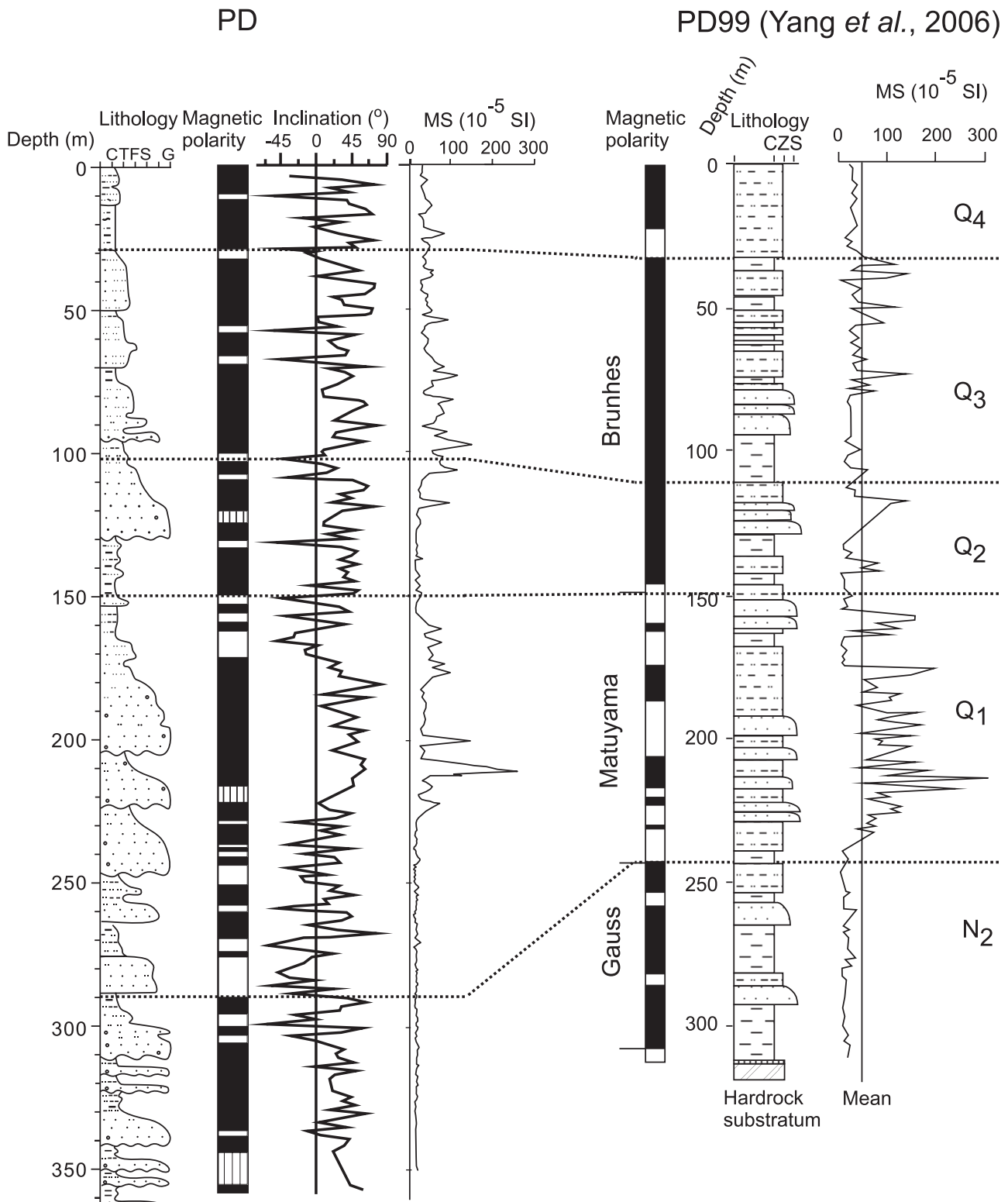
Vol. 3 No. 3

Jing Chen *et al.*: Clay minerals in the Pliocene−Quaternary sediments of
the southern Yangtze coast, China: Sediment sources and
palaeoclimate implications

303

Figure 4 Stratigraphic correlation between boreholes PD and PD99, including lithology, palaeomagnetism and magnetic susceptibility (MS). For lithological symbols, see Figure 3. Q_4−Holocene; Q_3−Late Pleistocene; Q_2−Mid-Pleistocene; Q_1−Early Pleistocene; N_2−Pliocene.

linite fluctuates between 13% and 0%, whereas chlorite is less than 6% in general. The crystallinity of illite is generally lower than 5.0, being the lowest in the whole core.

Suite II (287−248 m)

Illite increases in both proportion and crystallinity, but exhibits significant fluctuations in suite II. Its proportion ranges from 38% to 72%, with an average of 60%, whilst the H_w varies from 5.2 to 25.3, with an average of 20.1 (Figure 5). In contrast, smectite falls to 4%−31%, with an average of 17%. Kaolinite reaches its maximum among the 5 suites, ranging from 11% to 24%, with an average of 15% whilst chlorite increases to 5%−17%.

Suite III (245−155 m)

Illite dominates in suite III and becomes stable at about 65%, and H_w remains high at 21.3%−45.7% throughout (Figure 5). Chlorite becomes secondary, ranging from 7% to 23%, with an average of 16%. Kaolinite is the third in abundance, fluctuating between 6% and 15%. Smectite is the least, less than 7% in general, except a minor peak (~12%) in the top section.

Suite IV (155−130 m)

There are intensive oscillations in proportions of all clay minerals and H_w of illite in this transitional zone from the Early to Mid-Pleistocene (Figure 5). Illite still remains as the dominant component, but ranges from 38% to 85%, with an average of 63%. Its crystallinity declines significantly and appears as the second lowest (3.7%−37.1%) throughout the five suites. Smectite and kaolinite distinctly increase to 2%−36% and 9%−15%, respectively, while chlorite proportion is low with about 6%−13% in general, but with an increasing trend.

Suite V (130−0 m)

Illite is dominant and remains relatively stable in the Mid-Pleistocene to Holocene sediment of suite V at 55% to 82%, with an average of 71% (Figure 5). Chlorite becomes secondary again, varying between 11% and 25%, with an average of 16%. Kaolinite is steady at about 10% throughout, but with a slight increase in the Holocene sediment. Smectite is lower than 10%, with three small spikes throughout. The H_w values of illite get higher coin-
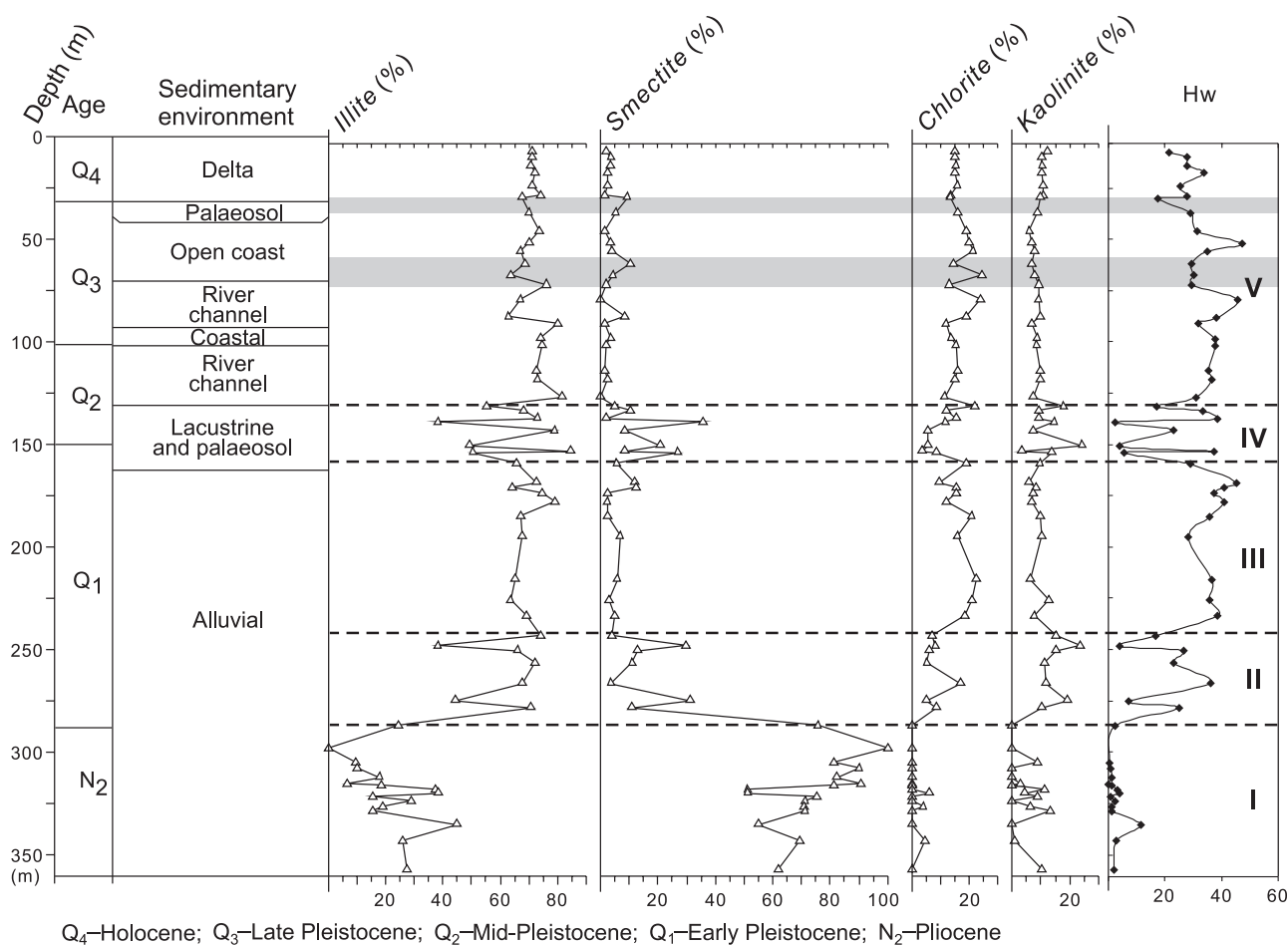

Figure 5 Vertical distribution of clay mineral proportions in borehole PD in relation to the sedimentary environment. Hw, the illite crystallinity, is defined as peak height/Kübler index.

Vol. 3 No. 3

Jing Chen *et al.*: Clay minerals in the Pliocene−Quaternary sediments of the southern Yangtze coast, China: Sediment sources and palaeoclimate implications

305

cidentally with its high proportion, and are characterized by a decreasing trend upward in the core and three lows in phase with the smectite peaks (Figure 5).

6 Discussion

Sediment provenance and climate implied by clay mineral

The predominance of smectite in suite I (Pliocene) suggests that the sediment source is primarily the local bedrock consisting of the Bai-Long-Gang basalt which flowed out during the Oligocene to Miocene (Qiu and Li, 2007). The dominant angular and subangular gravels (Table 2) point at a nearby source for the sediment. It is suggested that the study area was characterized by a strong relief and that only local small drainage basins developed at that time (Figure 2B), resulting in a very local sediment source in the present core area. The upward increase of smectite suggests that the climate became more arid during the Late Pliocene (Figure 5).

The illite-smectite featured in suite II indicates changes in both sediment source and palaeoclimate during the Early Pleistocene. The occurrence of the Bai-Long-Gang basalt is limited in the eastern Yangtze coastal plain, where its burial depth is generally >240 m beneath the present coastal surface (Wang *et al.*, 2008). Therefore, the basalt may have been mostly buried because of tectonic subsidence and associated sediment accumulation, so that there were mixed sediment sources. Round and semi-round gravels (Table 2) indicate that the basin where the borehole is located began to receive more sediments from the surrounding highlands. This change of the clay mineral assemblage could also be caused by a change of climate, *i.e.*, the glacial-interglacial cycles of the Early Pleistocene, as reflected by the strong fluctuations in the proportion and crystallinity of illite (Figure 5).

The obvious reduction of smectite in suite III indicates a significant change of sediment provenance and a further decrease in the contribution from local volcanic rocks. We thus suggest an expansion of drainage basin during the beginning of suite III. The thicker river channel deposits of suite III (Figure 3) indicate a prolonged river system with a larger catchment area. Our previous work on heavy minerals from borehole PD indicated a new sediment source of metamorphic rock from the middle to lower Yangtze drainage basin above a core depth of ~250 m (Chen *et al.*, 2009). The magnetic properties of the Late Cenozoic sediments in the study area further support the appearance of magnetite derived from metamorphic rock in the Early

Pleistocene (Wang *et al.*, 2008; Zhang *et al.*, 2009). This change of sediment source during the Early Pleistocene was also shown in a previous geochemical study of the nearby borehole PD99 (Yang *et al.*, 2006a, 2006b).

Suite IV of clay minerals represents the transitional phase from the Early to Middle Pleistocene when the environment was lacustrine (Figure 5). The dramatical fluctuation of smectite and kaolinite, along with the proportion and crystallinity of illite highlight distinctive alternations between chemical and physical weathering following the fluctuations of the palaeoclimate. This might be the record of the Mid-Pleistocene climate transition (MPT) at about 920−640 ka BP (Schmieder *et al.*, 2000; Zachos *et al.*, 2001; Raymo *et al.*, 2006), during which larger climate fluctuations occurred (Zheng *et al.*, 2005). Correspondently, this is also supported by lithologic evidence as layers of mottled muds that contain calcareous nodules and leaching structures defining buried palaeosols formed during glacial episodes (Figure 3). All these jointly reflect intensive glacial-interglacial cyclicities during the MPT, which allowed the deposition of lacustrine sediments during interglacials, and pedogenesis as it was exposed subaerially during the subsequent glacials. It is also suggested that the climate setting of the study area was characterized largely by contrasting seasonal conditions due to the intensified winter monsoon, which was caused by the rapidly increasing volume of the northern hemisphere ice-sheet during MPT (Ruddiman *et al.*, 1989; Berger *et al.*, 1999; Shackleton, 2000; Kitamura and Kawagoe, 2006). Such a climate is favorable for smectite formation accompanied by abundant kaolinite in pedogenic environments (Velde, 1992).

Smectite is, as a rule, rare in suite V after the MPT; it mostly amounts to 0−30% and never exceeds 10%, not even in the palaeosol (Figure 5). This is obviously less than the amount in suite III-IV (2%−36%). Illite predominates and appears to be highly crystallized in suite V (Figure 5), implying a temperate climate in the drainage basin. We suggest that the fine-grained sediment in suite V is similar to the presentday Yangtze muddy sediment which is also characterized by a low content of smectite (<5% in general; Liu *et al.*, 2006; Wang *et al.*, 2006). Chen *et al.* (2001) demonstrated that most of the presentday Yangtze suspended sediment discharging into the sea is derived from upstream, including the eastern Qinghai-Tibetan Plateau, where physical weathering prevails. Our previous studies on heavy minerals and magnetic minerals also revealed the supply of upstream sediment to the study area during the Late Pleistocene (Wang *et al.*, 2008; Chen *et al.*, 2009). The low values of illite crystallinity, accompanied by a

higher content of smectite might reflect the episodic subaerial exposure of former coastal/marine sediments during the later Pleistocene due to sea level fluctuations (Siddall *et al.*, 2003).

Tectonic subsidence and evolution of the east China marginal sea

The reduction of smectite and associated expansion of sediment provenance suggest tectonic subsidence at the borehole location during the Late Cenozoic. The changes of the sedimentary environment from an alluvial fan during the Pliocene and Early Pleistocene to an open coast and delta during the Late Pleistocene and Holocene also reflect significant tectonic subsidence of the study area (Chen and Stanley, 1995). Previous studies showed that the southern Yangtze coastal area remained as upland, presumably about 2000 m higher than the adjacent Subei-Southern YS Depression, during the Early Tertiary (Figure 2A). This is evident from the thick (2000−3000 m) Tertiary terrigenous deposits that occur in the depression (Wageman *et al.*, 1970; Chen and Stanley, 1995; Guo *et al.*, 1997). As the subsidence continued in the Wu-Nan-Sha and Fukien-Reinan Massifs during the Neogene and Quaternary, the study area has gradually became topographically lower from the Pliocene on. Meanwhile, the open coast environment and the arrival of Yangtze upstream sediments since the late stage of the Middle Pleistocene seems to imply the final submerge of the Wu-Nan-Sha and Fukien-Reinan Massifs (Figure 2A), which resulted in both the connection of the East China Sea and the southern Yellow Sea and the southward dispersal of Yangtze sediments. The submerge of the Fukien-Reinan Massif can also be concluded from the fact that marine influence only occurred in the Holocene and Late Pleistocene sediments in a Quaternary sediment core Ch1, located offshore of the Yangtze and on the Fukien-Reinan Massif (Qin *et al.*, 1987).

7　Conclusions

In conclusion, the smectite content serves as a diagnostic feature for the source of the sediments in borehole PD, whereas the content and crystallinity of illite, sensitive to climate change, records the strong fluctuations of the climate during the Early Pleistocene and MPT. This borehole documents a major expansion of the sediment source during the Early Pleistocene and a secondary change during the Mid-Pleistocene with a new source area from the upper Yangtze catchment area. The expansion of sediment source recorded in borehole PD implies tectonic subsidence of the study area and the coalition of the east China marginal sea

during Late Quaternary.

References

Aoki, S., Kohyama, N., 1991. The vertical change in clay mineral composition and chemical characteristics of smectite in sediment cores from the southern part of the Central Pacific Basin. Marine Geology, 98 (1): 41−49.

Berger, A., Li, X. S., Loutre, M. F., 1999. Modelling northern hemisphere ice volume over the last 3 Ma. Quaternary Science Reviews, 18, 1−11.

Biscaye, P. E., 1965. Mineralogy and sedimentation of the recent deep-sea clay in the Atlantic Ocean and adjacent seas and oceans. GSA Bulletin, 76: 803−832.

Chamley, H., 1989. Clay Sedimentology. Berlin: Springer, 1−623.

Chen, J., Wang, Z., Chen, Z., Wei, Z., Wei, T., Wei, W., 2009. Diagnostic heavy minerals in Plio-Pleistocene sediments of the Yangtze Coast, China with special reference to the Yangtze River connection into the sea. Geomorphology, 113: 129−136.

Chen, Z., Stanley, D. J., 1993. Alluvial stiff muds (Late Pleistocene) underlying the lower Nile delta plain, Egypt: Petrology, stratigraphy and origin. Journal of Coastal Research, 9 (2): 539−576.

Chen, Z., Stanley, D. J., 1995. Quaternary subsidence and river channel migration in the Yangtze delta plain, eastern China. Journal of Coastal Research, 11 (3): 927−945.

Chen, Z., Chen, Z. L., Zhang, W. G., 1997. Quaternary stratigraphy and trace element indices of the Yangtze delta, eastern China with special reference to marine transgression. Quaternary Research, 47: 181−191.

Chen, Z., Li, J., Shen, H., Wang, Z., 2001. Yangtze River of China: Historical analysis of discharge variability and sediment flux. Geomorphology, 41: 77−91.

Clark, M. K., Schoenbohm, L. M., Royden, L. H., Whipple, K. X., Burchfiel, B. C., Zhang, X., Tang, W., Wang, E., Chen, L., 2004. Surface uplift, tectonics, and erosion of eastern Tibet from large-scale drainage patterns. Tectonics, 23, TC1006, doi: 10.1029/2002TC001402.

Fan, D. J., Yang, Z. S., Mao, D., Guo, Z. G., 2001. Clay minerals and geochemistry of sediments from the Yangtze and Yellow Rivers.

Jing Chen *et al.*： Clay minerals in the Pliocene−Quaternary sediments of the southern Yangtze coast, China: Sediment sources and palaeoclimate implications

Vol. 3 No. 3

307

Marine Geology and Quaternary Geology, 21: 7−12 (in Chinese with English abstract).

Guo, Y. G., Li, Y. C., Xu, D. Y., Liu, X. Q., Zhang, X. H., 1997. Tectonic evolution of Yellow Sea, East China Sea continental shelf and adjacent areas. Marine Geology & Quaternary Geology, 17(1): 1−11 (in Chinese with English abstract)

He, L., Liu, Q., 1997. Chemical characteristics of clay minerals in the sediments from the Yellow River and the Changjiang River. Chinese Science Bulletin, 42: 488−492.

Jin, X. L., 1992. Marine Geology of the East China Sea. Beijing: Ocean Press, 524 (in Chinese).

Kitamura, A., Kawagoe, T., 2006. Eustatic sea-level change at the mid-Pleistocene climate transition: New evidence from the shallow-marine sediment record of Japan. Quaternary Science Reviews, 25: 323−335.

Li, C., Chen, Q., Zhang, J., Yang, S., Fan, D., 2000. Stratigraphy and paleoenvironmental changes in the Yangtze Delta during the Late Quaternary. Journal of Asian Earth Sciences, 18: 453−469.

Lin, J., Zhang, S., Qiu, J., Wu, B., Huang, H., Xi, J., Tang, B., Cai, Z., He, Y., 1989. Quaternary marine transgressions and paleoclimate in the Yangtze River delta region. Quaternary Research, 32(3): 296−306.

Liu, J. P., Li, A. C., Xu, K. H., Velozzi, D. M., Yang, Z. S., Milliman, J. D., DeMaster, D. J., 2006. Sedimentary features of the Yangtze River-derived along-shelf clinoform deposit in the East China Sea. Continental Shelf Research, 26(17−18): 2141−2156.

Liu, Z. F., Trentesaux, A., Clemens, S. C., Colin, C., Wang, P. X., Huang, B. Q., Boulay, S., 2003. Clay mineral assemblages in the northern South China Sea: Implications for East Asian monsoon evolution over the past 2 million years. Marine Geology, 201: 133−146.

Liu, Z. F., Colin, C., Trentesaux, A., Blamart, D., Bassinot, F., Siani, G., Sicre, M-A., 2004. Erosional history of the eastern Tibetan Plateau since 190 kyr ago: Clay mineralogical and geochemical investigations from the southwestern South China Sea. Marine Geology, 209: 1−18.

Ma, C., Chen, J., Zhou, Y., Wang, Z., 2010. Clay minerals in the major Chinese coastal estuaries and their provenance implications. Frontiers of Earth Science In China, 4: 449−456.

Madhavaraju, J., Ramasamy, S., Ruffell, Alastair, Mohan, S. P., 2002. Clay mineralogy of the Late Cretaceous and early Tertiary successions of the Cauvery Basin (southeastern India): Implications for sediment source and palaeoclimates at the K/T boundary. Cretaceous Research, 23: 153−163.

Naidu, A. S., Han, M. W., Mowatt, T. C., Wajda, W., 1995. Clay minerals as indicators of sources of terrigenous sediments, their transportation and deposition: Bering Basin, Russian-Alaskan Arctic. Marine Geology, 127: 87−104.

Pehlivanoglou, K., Tsirambides, A., Trontsios, G., 2000. Origin and distribution of clay minerals in the Alexandroupolis Gulf, Aegean Sea, Greece. Estuarine, Coastal and Shelf Science, 51 (1): 61−73.

Perederij, V. I., 2001. Clay mineral composition and palaeoclimatic interpretation of the Pleistocene deposits of Ukraine. Quaternary International, 76/77: 113−121.

Qin, Y. S., Zhao, Y. Y., Chen, L. Y., Zhao, S. L., 1987. Geology of the East China Sea. Beijing: Science Press, 290 (in Chinese).

Qiu, J., Li, X., 2007. Quaternary Stratigraphy and Sedimentary Environment of Shanghai. Shanghai: Shanghai Science and Technology Press, 1−230 (in Chinese).

Raymo, M. E., Lisiecki, L. E., Nisancioglu, K. H., 2006. Plio-Pleistocene ice volume, Antarctic climate, and global $\delta^{18}O$ record. Science, 313: 492−495.

Reading, H. G. (ed). 1996. Sedimentary Environments: Processes, Facies and Stratigraphy (3rd Ed.). Oxford: Blackwell Science Ltd., 688.

Ruddiman, W. F., Raymo, M. E., Martinson, D. G., 1989. Pleistocene evolution: Northern hemisphere ice sheet and North Atlantic Ocean. Paleoceanography, 4: 353−412.

Schmieder, F., Dobeneck, T., Bleil, U., 2000. The Mid-Pleistocene climate transition as documented in the deep South Atlantic Ocean: Initiation, interim state and terminal event. Earth and Planetary Science Letters, 179: 539−549.

Shackleton, N. J., 2000. The 100,000−year ice-age cycle identified and found to lag temperature, carbon dioxide, and orbital eccentricity. Science, 289: 1897−1902.

Shanghai Geological Survey, 2001. Geological Report of PD Borehole (unpublished report, in Chinese, 25).

Siddall, M., Rohling, E. J., Almogi-Labin, A., Hemleben, Ch., Meischner, D., Schmelzer, I., Smeed, D. A., 2003. Sea-level fluctuations during the last glacial cycle. Nature, 423(6942): 853−858.

Thorez, J., 1985. Argillogenesis and the hydrolysis index. Mineralogica et Petrographica Acta, 29: 313−338.

Vanderaveroet, P., Averbuch, O., Deconinck, J. F., Chamley, H., 1999. A record of glacial/interglacial alternations in Pleistocene sediments off New Jersey expressed by clay mineral, grain-size and magnetic susceptibility data. Marine Geology, 159: 79−92.

Velde, B., 1992. Introduction to clay minerals: Chemistry, origins, use and environmental significance. Chapman & Hall, London, 113−163.

Viscosi-Shirley, C., Mammone, K., Pisias N., Dymond, J., 2003. Clay mineralogy and multi-element chemistry of surface sediments on the Siberian-Arctic shelf: Implications for sediment provenance and grain size sorting. Continental Shelf Research, 23(11−13): 1175−1200.

Wageman, J. M., Hilde, T. W. C., Emery, K.O., 1970. Structural framework of East China Sea and Yellow Sea. AAPG Bulletin, 54: 1611−1643.

Wahsner, M., M. uller, C., Stein, R., Ivanov, G., Levitan, M., Shelekhova, E., Tarasov, G., 1999. Clay-mineral distribution in surface sediments of the Eurasian Arctic Ocean and continental margin as indictor for source areas and transport pathways—A synthesis. Boreas, 28: 215−233.

Walker, R. G., James, N. P., 1992. Facies Models: Response to Sea-Level Change. Ontario: Geological Association of Canada, 409.

Wang, P., 2004. Cenozoic deformation and the history of sea-land interactions in Asia. Geophysical Monograph Series, 149: 1−22.

Wang, Z., Chen, Z., and Tao, J., 2006. Clay mineral analysis of Yangtze delta, China, to interpret the late Quaternary sea-level fluctuations, climate change and sediment provenance. Journal of Coastal Research, 22 (3): 683−691.

Wang, Z., Zhang, D., Li, X., Tao, S., Xie, Y., 2008. Magnetic properties and relevant minerals of late Cenozoic sediments, Changjiang delta area and implications. Geology in China, 35(4): 670−682 (in Chinese with English abstract)

Wang, Z. H., Dong, Y. H., Chen, J., Li, X. F., Cao, J., Deng, Z. Y., 2014. Dating recent sediments from the subaqueous Yangtze Delta and adjacent continental shelf, China. Journal of Palaeogeography, 3(2): 207–218.

Wang, Z. Q., Chen, Z., Wei, Z. X., Wang, Z. H., Wei, T. Y., 2005. Coupling controls of Neotectonism and paleoclimate on the Quaternary sediments of the Yangtze (Changjiang) coast. Chinese Science Bulletin, 50 (16): 1775−1784.

Yang., Z. S., 1988. Mineralogical assemblages and chemical characteristics of clays from sediments of the Huang, Changjiang, Zhujiang rivers and their relationships to the climate environment in their sediment source areas. Oceanologia et Limnologia Sinica, 19 : 336−346 (in Chinese with English abstract)

Yang, S., Li, C., Cai, J., 2006a. Geochemical compositions of core sediments in eastern China: Implication for late Cenozoic palaeoenvironmental changes. Palaeogeography, Palaeoclimatology, Palaeoecology, 229: 287−302.

Yang, S., Li, C., Yokoyama, K., 2006b. Elemental compositions and monazite age patterns of core sediments in the Changjiang delta: Implications for sediment provenance and development history of the Changjiang River. Earth and Planetary Science Letters, 245: 762−776

Zachos, J., Pagani, M., Sloan, L., Thomas, E., Billups, K., 2001. Trends, rhythms, and aberrations in global climate 65 Ma to present. Science, 292: 686−693.

Zhang, D., Wang, Z., Wei, W., Li, X., 2009. Rock magnetic properties and source indications of late Cenozoic sediments in Yangtze delta area. Quaternary Sciences, 29(2): 308−217 (in Chinese with English abstract).

Zhang, Y., Xue, Y. Q., Wu, J. C., Yu, J., Wei, Z. X., Li, Q. F., 2008. Land subsidence and earth fissures due to groundwater withdrawal in the southern Yangtze delta, China. Environmental Geology, 55: 751−762.

Zhao, B., Wang, Z., Chen, J., Chen, Z., 2008. Marine sediment records and relative sea level change during late Pleistocene in the Changjiang delta area and adjacent continental shelf. Quaternary International, 186: 164−172.

Zheng, F., Li, Q., Li, B., Chen, M., Tu, X., Tian, J., Jian, Z., 2005. A millennial scale planktonic foraminifer record of the mid-Pleistocene climate transition from the northern South China Sea. Palaeogeography, Palaeoclimatology, Palaeoecology, 223: 349−363.

(Edited by Yuan Wang)